IEEE Access
Multidisciplinary | Rapid Review | Open Access Journal

Received September 17, 2020, accepted October 4, 2020, date of publication October 9, 2020, date of current version October 29, 2020.

Digital Object Identifier 10.1109/ACCESS.2020.3029839

ECT Sensor Simulation and Fuzzy Optimization Design Based on Multi Index Orthogonal Experiment

ZHE JI, (Graduate Student Member, IEEE), JIANYU LIU, HAIJUN TIAN, (Member, IEEE), AND WANG ZHANG
School of Automation Engineering, Northeast Electric Power University, Jilin 132012, China

Corresponding author: Haijun Tian (13944242775@139.com)

This work was supported by the national key research and development program of gas-liquid two-phase flow parameter measurement instrument, under Grant 2018YFF01013801.

ABSTRACT Electrical Capacitance Tomography (ECT) is a non-destructive visual measurement technology, which is mainly used in the detection of two-phase flow and multi-phase flow. In this paper, according to the characteristics of the non-uniform sensitive field and the low sensitivity of the central area of the capacitance sensor, the finite element simulation analysis in COMSOL and the orthogonal test design method are introduced to optimize the structural parameters of the capacitance sensor, including the geometric size of the electrode plate, the height of the shield, the thickness of the pipe wall and its relative permittivity. In view of the analytical relationship between the structural parameters and the performance optimization indexes of the capacitance sensor, and there are many parameters need to be optimized, this paper proposes a fuzzy comprehensive satisfaction index (FCSI) as the evaluation standard, and on this basis carries out the optimization design of the structural parameters of the capacitance sensor. The simulation results show that the fuzzy optimization design based on multi index orthogonal experiment makes the capacitance sensor meet the requirements of uniform sensitive field distribution and high reconstruction image quality at the same time.

INDEX TERMS Electrical capacitance tomography, fuzzy analysis, finite element analysis, orthogonal test, sensitive field.

I. INTRODUCTION

Multi-phase flow is widely used in petrochemical, metallurgy, electric power, energy and other industrial production fields, and its related process parameters detection is very important for the accurate control of the production process and ensure the production safety and efficiency [1], [2]. Compared with single-phase flow, the flow mechanism and mathematical model of multi-phase flow are very complex, which makes the accurate detection of phase holdup, phase velocity, concentration and flow pattern of multi-phase flow become a difficult problem for industry [3]. Because traditional detection technology is difficult to measure accurately, it is necessary to study a stable, simple structure and easy-to-implement non-invasive visual detection technology [4], [5].

The associate editor coordinating the review of this manuscript and approving it for publication was Wuliang Yin.

Electrical capacitance tomography technology is one of these technologies. This technology has been widely used in industrial production processes, such as the monitoring of the ratio of pulverized coal to air and the flow rate during the pneumatic transportation of pulverized coal in pipelines [6], [7]; During the transmission of crude oil and natural gas industry, the monitoring field of oil-water and oil-gas two-phase flow, and the accurate measurement of the oil holdup, gas holdup and other components holdup and distribution [8]. A large number of industrial processes put forward higher requirements for the detection of process parameters related to multiphase flow [9].

According to the characteristics of ''soft field'' in ECT sensor, the sensitive field distribution is non-uniform, the sensitivity near the polar plate is higher, and the sensitivity at the center of the field is lower, which has a great influence on the quality of the reconstructed image. To optimize the structural parameters of the ECT sensor, thereby improving

the sensitive field distribution and improving the quality of the reconstructed image. This paper introduces the method of combining finite element analysis and orthogonal experimental design to optimize the design of the structural parameters that affect the performance of the capacitance sensor, so that the order of the primary and secondary effects of each factor can be determined without passing all the experiments. Based on the related concepts of fuzzy mathematics, this paper proposes a fuzzy analysis method of multi-index orthogonal experiment to comprehensively evaluate the performance of capacitive sensors, using COMSOL finite element simulation software to simulate, make the sensitive field distribution more uniform, and reduce the medium distribution Influence, the media distribution reconstructed from the capacitance measurement value can reflect the original image more accurately.

II. BASIC THEORY OF ECT SYSTEM

A. ECT SYSTEM COMPOSITION STRUCTURE AND WORKING PRINCIPLE

The physical basis of electrical capacitance tomography measurement is to use the different dielectric constants of the phases of the multiphase flow medium to be measured. When the distribution of each phase of the medium or the concentration of each phase changes, the mixed dielectric of the multiphase flow will change. The capacitance value measured by the array electrode of the ECT sensor changes accordingly. The capacitance value between the electrode plate pairs is used to solve the medium distribution in the pipe or the insulated closed container, thereby reconstructing the multiphase flow medium distribution image [10]. The ECT sensor is mainly composed of an insulated pipe, a copper measuring electrode plate arrays that provides the required data for reconstructed images, a radial electrode installed between adjacent electrode plate arrays, and a ground shield installed to prevent interference from the external electromagnetic field on the electrode arrays cover composition. At present, the number of plates of commonly used ECT system sensors are 8, 12, 16, etc.

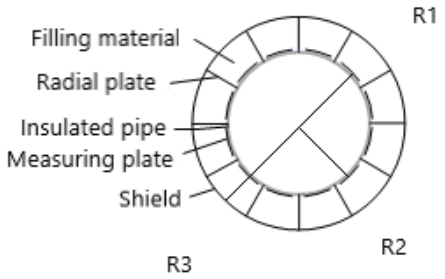

FIGURE 1. Cross-sectional structure diagram of a capacitive sensor.

B. MATHEMATICAL MODEL OF ECT SYSTEM

Because the excitation power supply of ECT system is low frequency power supply, it meets the condition of electrostatic field [11]. The mathematical model of ECT system can be described as follows:

$$\nabla \cdot D = \rho \tag{1}$$

where D is electric displacement, C/m^2; ρ is the charge density, C/m^3.

According to the relationship between electric field strength and electric potential energy, the electric field strength is the negative gradient of the electric potential energy function. We get the following results:

$$\nabla \cdot D = \nabla \cdot \varepsilon E = \nabla \cdot (\varepsilon \cdot (-\nabla \phi)) = \rho \tag{2}$$

where E is the electric field strength, V/m; ε is the relative permittivity of the measured medium in the field.

Due to the low frequency excitation, there is no isolated charge in the measured area. The forward problem of ECT system belongs to the first kind of boundary value problem, so the forward problem model can be expressed by Laplace equation of electrostatic field:

$$\nabla \cdot [\varepsilon(x, y) \nabla \phi(x, y)] = 0 \tag{3}$$

Taking 12 electrodes as an example, when the electrode plate is used as the excitation electrode plate, the Dirichlet boundary condition equation is obtained as:

$$\phi(x, y) = \begin{cases} U & (x, y) \subseteq \Gamma_i \\ 0 & (x, y) \subseteq \Gamma_j \, (j = 1, 2, \ldots, 12, j \neq i) \cap \\ & (x, y) \subseteq \left(\Gamma_s + \Gamma_{pg}\right) \end{cases} \tag{4}$$

where U is the boundary excitation voltage; $\Gamma_1, \Gamma_2, \ldots, \Gamma_{12}$ are the spatial positions where the 12 pole plates are located; Γ_s, Γ_{pg} are the positions of the ground barrier cover and the radial electrode position respectively.

C. SENSITIVE FIELD CALUATION

According to the Gaussian flux theorem, the amount of induced charge on the detection plate j can be calculated as:

$$Q_{ij} = \oint_{\Gamma_j} \varepsilon_0 \varepsilon \, (x, y) \, E \hat{n} dl = - \oint_{\Gamma_j} \varepsilon_0 \varepsilon \, (x, y) \, \nabla \phi(x, y) \cdot \hat{n} dl \tag{5}$$

where Q_{ij} is the amount of induced charge on the electrode plate,Γ_j is the enclosed area surrounding the detection plate j, ε_0 is the vacuum dielectric constant, n is the unit normal vector on the enclosed area.

The electrode plate i of ECT sensor is the excitation plate, and the electrode Plate j is the capacitance value when the electrode plate is detected, In the case of known potential distribution $\phi \, (x, y)$, it can be calculated from equation (6):

$$C_{ij} = \frac{Q_{ij}}{U_{ij}} = -\frac{1}{U} \iiint_{\Gamma} \varepsilon(x, y) \nabla \phi(x, y) \hat{n} dl \tag{6}$$

where U_{ij} is the potential difference between the plates.

According to the above formula, there is a nonlinear relationship between the measured capacitance C and the distribution of ε relative permittivity, which can be expressed as:

$$C = F(\varepsilon) \tag{7}$$

Sensitivity matrix is needed in the reconstruction of dielectric constant distribution [12], [13], The formula is as follows:

$$S_{ij}(\sigma) = \frac{\Delta C_{ij}}{\Delta \varepsilon} \approx -\frac{\int \nabla \phi_i \cdot \nabla \phi_j ds}{U^2} \tag{8}$$

Regarding area σ as the pixels of the image, the sensitive field distribution on each pixel in the measured area can be calculated by equation (8).

III. PERFORMANCE EVALUATION INDEX OF ECT SENSOR

In electrical capacitance tomography system, the distribution of sensitive field is uneven. In order to make the sensitive field of ECT sensor more uniform, it is usually necessary to optimize the sensor parameters.

A. OPTIMIZATION OBJECTIVE FUNCTION OF SENSITIVITY FIELD UNIFORMITY

1) UNIFOEMITY OF SENSITIVITY DISTRIBUTION

Sensitivity uniformity is an important optimization index for capacitive sensor parameters design [14]. Because of the symmetry of the 12 electrode ECT system, only six different sensitivity distributions need to be considered, which is $S_{i,j}\,(i = 1, j = 2, \ldots, 7)$. The average sensitivity $S_{i,j}^{avg}$ and standard deviation $S_{i,j}^{dev}$ of n micro-elements in the measured area are as follows:

$$\begin{cases} S_{i,j}^{avg} = \dfrac{1}{n}\displaystyle\sum_{e=1}^{n} S_{i,j}(k) \\ S_{i,j}^{dev} = \left\{ \dfrac{1}{n-1}\displaystyle\sum_{e=1}^{n}\left[S_{i,j}(k) - S_{i,j}^{avg}\right]^2 \right\}^{1/2} \end{cases} \tag{9}$$

At this time, a capacitance sensor optimization index is introduced to measure the uniformity of sensitivity distribution.

$$P = \frac{1}{6}\left(\sum_{i=1}^{}\sum_{j=2}^{7}\left|\frac{S_{i,j}^{dev}}{S_{i,j}^{avg}}\right|\right) \tag{10}$$

In the formula, the smaller the value of P, the more uniform the sensitivity distribution between the plate pairs.

2) DYNAMIC RANGE OF CAPACITANCE MEASUREMENT

Define the capacitance dynamic range k_c as the ratio of the maximum capacitance value $C_{\max}$ when measuring the full field between the plates to the minimum capacitance value $C_{\min}$ when measuring the empty field:

$$k_c = \frac{C_{\max}}{C_{\min}} \tag{11}$$

The value of k_c in the formula should not be too large.

3) SENSITIVITY OF CAPACITANCE MEASUREMENT

The sensitivity of capacitance measurement is defined as the ratio of the difference ΔC between the full-field and the empty-field capacitance measured between the plates to the capacitance value C^l during the empty-field measurement:

$$\frac{\Delta C}{C} = \frac{C_{i,j}^h - C_{i,j}^l}{C^l} \tag{12}$$

The higher the value of $\Delta C/C$, the higher the sensitivity of capacitance measurement

According to the analysis of these three indicators, the optimal design of capacitance sensor parameters is a multi-input optimization process. The weighted combination of functions is defined as the objective function $T(X)$ for optimizing the uniformity of the sensitive field, which is taken as the objective of optimizing the sensitive field of the ECT sensor:

$$T(X) = k_c + \alpha\frac{C}{\Delta C} + \beta P \tag{13}$$

where α and β are weight coefficients, This article chooses $\alpha = 0.47, \beta = 0.7$ refer to the reference [9] and reference [15]. X is the structure parameter vector. When the value of $T(X)$ is smaller, the performance of the capacitive sensor is better. Therefore, the problem of ECT sensor parameter optimization is transformed into the problem of finding the minimum value of function $T(X)$ in the defined domain.

B. RELATIVE IMAGE ERROR

The relative error ε_{image} of the reconstructed image is defined as:

$$\varepsilon_{image} = \frac{\|g - \hat{g}\|}{\|\hat{g}\|} \tag{14}$$

where g is the true value of the dielectric constant distribution;$\hat{g}$ is the calculated value of the dielectric constant distribution.

The quality of the reconstructed image during the structural optimization of the capacitive sensor can objectively reflect the performance of the sensor. In this paper, the image reconstruction of two-phase laminar flow with 1/4 inner diameter height is carried out. The filtering linear back projection imaging algorithm is used to select the relative error ε_{image} value as the evaluation index. The relative permittivity of the phase with high and low permittivity is set to be 3 and 1 respectively.

C. FUZZZY COMPREHENSIVE SATISFACTION

In the orthogonal experiment of single optimization index, the intuitive analysis method can quickly draw conclusions. However, in orthogonal experiments with multiple optimization indicators, there are often contradictions among multiple indicators. Optimizing indicators $T(X)$ and ε_{image} are selected as optimization indicators. The experimental results have completely different dimensions and physical meanings,

which makes it difficult to evaluate the experimental program. If the weight distribution method is used to combine the two, the corresponding membership function should be constructed to map the numerical results of $T(X)$ and ε_{image} as evaluation indexes to the same set interval. Aiming at the orthogonal experiment of multiple optimization indexes, this paper uses the related concepts of fuzzy mathematics and the concept of comprehensive satisfaction. Based on the establishment of the comprehensive satisfaction index, the fuzzy analysis method of multi-index orthogonal experiment is established. Define the fuzzy comprehensive satisfaction index (Fuzzy Comprehensive Satisfaction Index, FCSI) to evaluate the performance of ECT sensors.

In the orthogonal experiment process of multiple optimization evaluation indexes, if n evaluation indexes $A_j(j = 1, 2, \ldots, n)$ are set, the universe X is formed by all index sets. A certain experiment is recorded as experiment i, and the value of evaluation index A_j obtained is recorded as $x_{i,j}(i = 1, 2, \ldots, m)$, which is the element contained in X.

For any $x_{i,j} \in X$, the following mapping form is given.

$$\begin{aligned} X &\mapsto [0, 1] \\ x_{i,j} &\mapsto \mu_{A_j}(A_j) \in [0, 1] \end{aligned} \tag{15}$$

Then call the set composed of the following ''order pairs'' as the fuzzy set on X.

$$\tilde{A}_j = \{(x_{i,j} \big| \mu_{A_j}(x_{i,j}))\}, \forall x_{i,j} \in X \tag{16}$$

For a specific $x_{i,j}$, the value of membership function $\mu_{A_j}(x_{i,j})$ is called $x_{i,j}$'s satisfaction with A_j index of $\tilde{A}_j$. If $\mu_{A_j}(x_{i,j}) = 1$, it is said that $x_{i,j}$ is completely subordinate to $\tilde{A}_j$, indicating satisfaction. If $\mu_{A_j}(x_{i,j}) = 0$, it means that $x_{i,j}$ is not affiliated to $\tilde{A}_j$ at all, indicating dissatisfaction.

Some known functions can be used to describe the acceptance level of indicator changes. Taking the normal

function as an example, the commonly used evaluation index satisfaction functions constructed have the following types.

1) LARGE INDICATORS, USING THE ASCENDING HAIF-NORMAL DISTRIBUTION AS FUNCTION AS SHOWN IN EQUATION (17):

$$\mu_{A_j}(x_{i,j}) = \begin{cases} 0 & x_{i,j} \le a \\ 1 - e^{-k(x_{i,j}-a)^2} & x_{i,j} > a \end{cases} \tag{17}$$

where is $K > 0$.

When the index value is $x_{i,j} \le a$, the result is considered completely unacceptable, that is, completely unsatisfactory; when the index value is $x_{i,j} > a$, as the index value increases, satisfaction shows a normal upward trend, until the result is completely acceptable.

The coefficient K determines the link between the index value and the acceptability. Its determination method includes direct determination by empirical method; or multiple experiments are carried out to select the index value according to certain principles (median point, extreme point, frequency of repeated occurrence, etc.), determine the value of corresponding satisfaction function, and then calculate the coefficient K by statistical analysis.

2) PARTIALLY SMALL INDICATORS, USING THE REDUCED HALF NORMAL DISTRIBUTION FUNCATION AS SHOWN IN EQUATION (18):

$$\mu_{A_j}(x_{i,j}) = \begin{cases} 1 & x_{i,j} \le a \\ e^{-k(x_{i,j}-a)^2} & x_{i,j} > a \end{cases} \tag{18}$$

where is $K > 0$.

When the index value is $x_{i,j} \le a$, the result is considered to be completely acceptable, that is, completely satisfied with the result; when the index value is $x_{i,j} > a$, with the increase of the index value, the satisfaction rate shows a normal downward trend.

3) THE INTERMEDIATE INDEX IS SHOWN IN EQUATION (19) BY USING NORMAL DISTRIBUTION FUNCTION

$$f_{A_j}(x_{i,j}) = \begin{cases} 0 & x_{i,j} \le a \\ e^{-k(x_{i,j}-c)^2} & a < x_{i,j} < b \\ 0 & x_{i,j} \ge b \end{cases} \tag{19}$$

where is $K > 0, c \in (a, b)$. The constant c represents the ideal value of the index.

When the index is $x_{i,j} \in (a, b)$, the satisfaction is normally distributed; when the index value is $x_{i,j} \notin (a, b)$, the result is considered completely unacceptable, that is, completely dissatisfied.

The index comprehensive satisfaction function shows how close each index value is to the concept of satisfaction in an experiment conducted, that is, how close the overall performance effect of this experiment is to the concept of satisfaction. The index comprehensive satisfaction function has a variety of construction methods, and the vector single value method is used in this article.

In the orthogonal experiment of multi-index optimization, in a certain experiment i, the satisfaction set of each evaluation index obtained as follows:

$$\tilde{B}_i = \{(x_{i,j} \big| \mu_{A_{i,j}}(x_{i,j})), j = 1, 2, \ldots, n, i = 1, 2, 3, \ldots, m\} \tag{20}$$

Y is a special Set.

For any $\tilde{B}_i \in Y$, the following mapping is given.

$$\begin{aligned} Y &\mapsto [0, 1] \\ \tilde{B}_i &\mapsto g(\tilde{B}_i) \in [0, 1] \end{aligned} \tag{21}$$

Then the set composed of the following ''order pairs'' is called the fuzzy set on Y.

$$\tilde{C} = \{(\tilde{B}_i \Big| g(\tilde{B}_i))\}, \forall \tilde{B}_i \in Y \tag{22}$$

The membership function $g(\tilde{B}_i)$ is called the comprehensive satisfaction function of the evaluation index of $\tilde{B}_i$ versus $\tilde{C}$. For a specific $\tilde{B}_i$, $g(\tilde{B}_i)$ is called $\tilde{B}_i$'s comprehensive satisfaction with the index in Experiment i of $\tilde{C}$. If $g(\tilde{B}_i) = 1$,

TABLE 1. Experimental factors and their levels.

Factor level	Electrode opening angle (°)	Relative thickness of pipe wall	Relative height of shield	Dielectric constant of tube wall
Level 1	15	0.08	1.4	2
Level 2	18	0.12	1.6	3
Level 3	21	0.16	1.8	4
Level 4	24	0.20	2.0	5

it is said that $\tilde{B}_i$ is completely subordinate to $\tilde{C}$, which means satisfaction. If $g(\tilde{B}_i) = 0$, it is said that $\tilde{B}_i$ does not belong to $\tilde{C}$ at all, which means that it is not satisfied.

Two methods, weighted arithmetic average method and weighted geometric average method, can be used for single-valued representation of vectors [15]. This paper uses the weighted arithmetic average method to construct a comprehensive satisfaction function.

In the multi index orthogonal experiment, W_j is used to represent the relative importance of performance index $A_j(j = 1, 2, \ldots, n)$, which meets the following requirements:

$$\sum_{j=1}^{n} w_j = 1(w_j \geq 0) \tag{23}$$

Then the weighted arithmetic average is used to obtain the following results:

$$g(\tilde{B}_i) = \sum_{j=1}^{n} w_j \mu_{A_j}(x_{i,j})(i = 1, 2, 3, \ldots, m) \tag{24}$$

Similarly, using weighted arithmetic average, we can get the following results:

$$g(\tilde{B}_i) = \prod_{j=1}^{n} [\mu_{A_j}(x_{i,j})]^{w_j}(i = 1, 2, 3, \ldots, m) \tag{25}$$

From the value of $g(\tilde{B}_i)$, the comprehensive satisfaction value in experiment i can be obtained, so the orthogonal experiment of multi-index optimization is transformed into the orthogonal experiment of single-index optimization. Through the numerical value of previous experiment $g(\tilde{B}_i)$, the various factors of the experiment are visually analyzed to determine the optimal scheme of the experiment and obtain the optimized structural parameters of the capacitive sensor.

According to the results of the orthogonal experiment, a small index satisfaction function is constructed by using formula (21), and the function formula of membership of $T(X)$ and ε_{image} is obtained:

$$\mu_T(x, y) = \begin{cases} 1 & x_{i,j} = 0 \\ e^{-0.00153x_{i,j}^2} & x_{i,j} > 0 \end{cases} \tag{26}$$

$$\mu_\varepsilon(x, y) = \begin{cases} 1 & x_{i,j} = 0 \\ e^{-5.2453x_{i,j}^2} & x_{i,j} > 0 \end{cases} \tag{27}$$

Therefore, the fuzzy comprehensive satisfaction optimization index FCSI in experiment i is constructed.

$$FCSI(x_{i,j}) = \frac{1}{2}e^{-0.00153x_{i,1}^2} + \frac{1}{2}e^{-5.2453x_{i,2}^2} \tag{28}$$

IV. OPTIMAL DESIGN OF ECT SENSOR

A. DESIGN OF ORTHOGONAL EXPERIMENT SCHEME OF ECT SENSOR

The structural parameters of the capacitive sensor mainly include the opening angle θ of the electrode plate, the pipe wall thickness $R_2 - R_1$ of the insulated pipe and the dielectric constant ε_w of the filling material, the thickness of the shielding layer, which is the distance $R_3 - R_2$ between the ground shielding cover and the electrode plate, and the insertion depth h of the radial electrode. Generally, for different working conditions, the inner diameter of the measuring pipe is different. In this paper, the inner radius of the pipe is selected as $R_1 = 50$mm. Due to the difference of shield thickness caused by the uncertainty of pipe wall thickness, the above parameters related to the inner radius of pipeline are normalized [16], [17], which is $Z_1 = R_2 - R_1/R_1$, $Z_2 = R_3/R_1$.

According to the actual needs of the electrical capacitance tomography system, the optimal design parameters of the capacitance sensor are selected. The experimental factors and their levels are shown in Table 1. For a problem with a factor of 4 and a level of 4, it takes 256 times to perform all experiments. However, using the 4-level orthogonal table L16 to carry out the orthogonal experimental design of the capacitive sensor only requires 16 times. Under the premise of ensuring the objective results of the experiment, the number of experiments can be effectively reduced.

B. THE INFLUENCE OF RADIAL ELECTRODE ON SENSOR PERFORMANCE

Whether the ECT sensor is equipped with radial electrode and whether the radial electrode is embedded in the pipe wall has a significant impact on the sensor characteristics and the distribution of sensitive field. In our experimental simulation process, we found that whether the radial electrode is installed and whether the radial electrode is embedded in the pipe wall has a greater impact on the sensitive field distribution of laminar flow, so we choose laminar flow to verify the imaging error.

Fig. 2 shows the vector distribution diagram of the electric field lines in the ECT sensor without radial electrodes

(a) Distribution of electric field line vector without radial electrode (b) Distribution of electric field line vector with radial electrode

FIGURE 2. Distribution of electric field line vector.

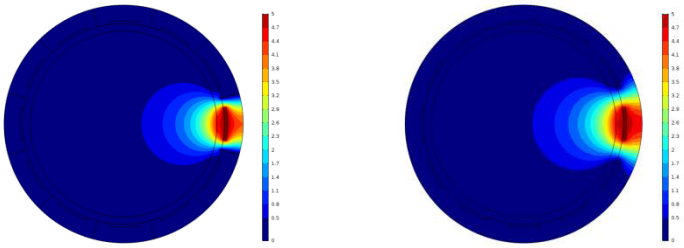

(a) Distribution of equipotential lines without radial electrodes (b) Equipotential distribution with radial electrodes

FIGURE 3. Distribution of equipotential lines.

and with radial electrodes. Fig. 3 shows the distribution of equipotential lines in an ECT sensor without and with radial electrodes.

It can be seen from Fig. 2 and 3 that the electric field lines from the excitation plate reach the detection plate through the inside of the pipe and the shielding layer area. The electric field distribution in the area of the pipeline is weakly affected by whether the radial electrode is installed or not, but the electric field line distribution on the outside of the electrode plate is more affected. With or without radial electrodes, the trend of electric field line vector distribution and equipotential line distribution is basically the same. However, the equipotential lines and electric field distribution between the shielding layers are cut off due to the installation of the radial electrode.

The main functions of radial electrodes in ECT sensors are reflected in the following aspects:

1) REDUCE THE CAPACITANCE BETWEEN ADJACENT PLATES

According to Gauss theorem, starting from the excitation plate, the greater the ''number'' of electric field lines arriving at the detection plate, the greater the amount of electric charge induced, thus the greater the capacitance between the plates. Therefore, the measured capacitance is directly proportional to the number of electric field lines arriving at the detection plate. The ECT sensor with radial electrodes causes the electric field lines from the outside of the pipe to the adjacent detection plates to be cut, thereby reducing the measured capacitance between adjacent plates. The electric field lines that reach the detection plate from the inside of the pipeline are not affected. Therefore, the radial electrode has little effect on the capacitance value between the plates that are far away.

2) REDUCE THE DYNAMIC RANGE OF CAPACITANCE

Because the capacitance between adjacent plates is mainly affected by the electric field near the plates; while the capacitance between the plates with a long distance is mainly affected by the distribution of dielectric constant in the pipeline; the capacitance between adjacent plates is much smaller than that between other non-adjacent plates due to the installation of radial electrodes. The radial electrode is embedded in the pipe so that the capacitance value between the plates is reduced more than if it is not embedded in the pipe. This is due to the embedding of radial electrodes, which reduces the number of electric field lines reaching the detection plate, and the capacitance between the plates decreases more. Therefore, the dynamic range of capacitance can be reduced by installing radial electrode.

3) IMPROVE SENSOR SENSITIVE FIELD DISTRIBUTI

The influence of different conditions of installation of radial electrodes on the sensitive field distribution is shown in Fig. 4 and Fig. 5. It can be seen from the figure that when there is no radial electrode, the sensitive field between adjacent plates (The range of change reflected in the vertical axis) is stronger. The intensity of the sensitive field gradually weakens with the installation of the radial electrode and the intensity of the embedded tube wall. For the sensitive field between the opposite plates, as the radial electrode is installed and embedded in the tube wall, the sensitive field gradually weakens near the radial electrode, but the sensitive field in the pipeline is enhanced. The sensitive field between non-adjacent plates is similar to the sensitive field between opposite plates. Therefore, the installation of radial electrodes can effectively weaken the sensitive field between

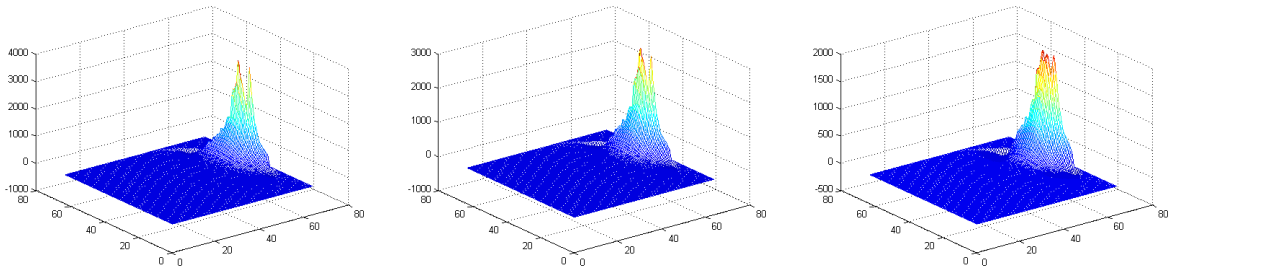

(a) No radial electrode (b) Radial electrodes are installed outside the tube wall (c) Radial electrodes embedded in the tube wall

FIGURE 4. Sensitivity distribution between adjacent plates.

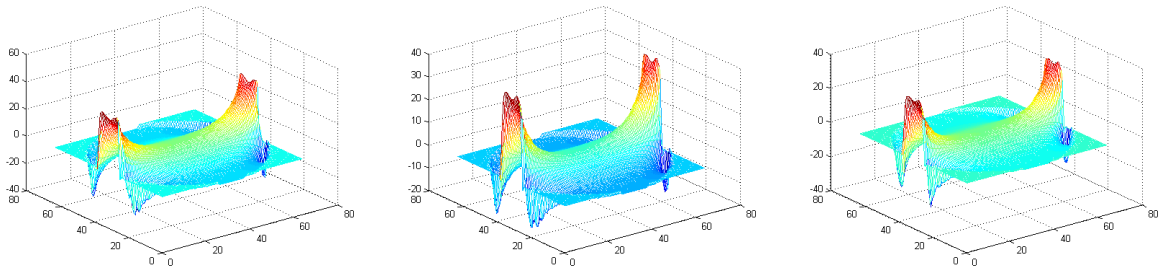

(a) No radial electrode (b) Radial electrodes are installed outside the tube wall (c) Radial electrodes embedded in the tube wall

FIGURE 5. Sensitivity distribution between relative plates.

adjacent plates of the capacitive sensor and increase the sensitive field between non-adjacent plates of the capacitive sensor. Therefore, the problem of uneven sensor field distribution is improved, and the quality of image reconstruction is improved.

C. OPTIMIZATION RESULTS OF ECT SENSORS PARAMETERS

Due to the existence of the "soft field" characteristic, in the analysis of the influence of the structural parameters of the capacitive sensor on the optimization index, only a single parameter of the sensor structure is changed in each experimental process, and the influence of multiple factors on the performance cannot be comprehensively investigated. Therefore, it is necessary to comprehensively consider the various factors of the sensor, and perform simulation experiments to optimize the search for the optimal parameters, so that better reconstructed images can be obtained. The sensitivity field uniformity optimization objective function $T(X)$, relative error ε_{image} and fuzzy comprehensive satisfaction index (FCSI) are selected as optimization indexes. For three different optimization indexes, orthogonal design method is used to arrange experiments. Orthogonal experiment scheme and its experimental results are shown in Table 2.

The analysis of the results of orthogonal experiment shows that when one index is optimal, the result of the other index is not optimal. There is a certain contradiction between the two optimization conditions as the optimization objective.

The range analysis of the orthogonal test results is shown in Table 3.

In the Table 3, RT is the range of the sensitive field uniformity optimization objective function $T(X)$, R_ε is the range of the relative error index ε_{image}, and R is the range of the fuzzy comprehensive satisfaction index FCSI. Use A to indicate the opening angle of the pole plate, B to indicate the relative thickness of the tube wall, C to indicate the relative height of the shielding cover, and D to indicate the dielectric constant of the tube wall. For example, $A_1B_2C_3D_4$ means that when the optimization index is a certain function, among the four sets of analysis data, select the data of the first set of plate opening angle, select the data of the second set of relative tube wall thickness, select the data of third set of shield height and the fourth group of data of the wall dielectric constant are used as the optimal combination. It can be seen from Table 3 that when the optimization index is $T(X)$, the optimal combination is $A_1B_3C_1D_3$, and the primary and secondary order of the influence of the four optimization experimental factors on $T(X)$ is B>C>A>D. When the optimization index is ε_{image}, the optimal combination is $A_4B_3C_4D_3$, and the primary and secondary order of the influence of the 4 optimization experimental factors on ε_{image} is B>C>A>D. When the optimization index is FCSI, the optimal combination is $A_4B_3C_1D_3$, and the primary and secondary order of the influence of the four optimization experimental factors on FCSI is B>C>A>D.

As an optimized combination plan that was not arranged in the simulation test plan was obtained, an experiment was

TABLE 2. Orthogonal experiment scheme and experimental results.

Experiment	Experimental parameters				Calculation results		
number	Electrode opening angle (°)	Relative thickness of pipe wall	Relative height of shield	Dielectric constant of tube wall	$T(X)$	ε_{image}	FCSI
1	15	0.08	1.4	2	5.022943	0.37841	0.716903
2	15	0.12	1.6	3	4.891139	0.36761	0.728054
3	15	0.16	1.8	4	4.941373	0.3474	0.747068
4	15	0.20	2.0	5	5.384574	0.3551	0.736265
5	18	0.08	1.6	4	5.244377	0.37214	0.721121
6	18	0.12	1.4	5	4.92371	0.36527	0.730041
7	18	0.16	2.0	2	5.126887	0.34434	0.748651
8	18	0.20	1.8	3	5.455423	0.42619	0.670479
9	21	0.08	1.8	5	5.437951	0.37358	0.718241
10	21	0.12	2.0	4	5.064149	0.36562	0.72867
11	21	0.16	1.4	3	4.8595	0.35899	0.736502
12	21	0.20	1.6	2	5.763046	0.57143	0.565295
13	24	0.08	2.0	3	5.472636	0.37433	0.717257
14	24	0.12	1.8	2	4.985366	0.3733	0.721983
15	24	0.16	1.6	5	4.877196	0.35898	0.736384
16	24	0.20	1.4	4	4.999529	0.33767	0.756086

TABLE 3. Range analysis of orthogonal test results.

Index	Polar plate opening angle (°)	Relative thickness of pipe wall	Relative height of shield	Dielectric constant of tube wall
K_{T1}	5.060007	5.294477	4.951421	5.224561
K_{T2}	5.187599	4.966091	5.19394	5.169675
K_{T3}	5.281162	4.951239	5.205028	5.062357
K_{T4}	5.083682	5.400643	5.262062	5.155858
R_T	0.221154	0.449404	0.310641	0.090755
$K_{\varepsilon 1}$	0.36213	0.374615	0.360085	0.41687
$K_{\varepsilon 2}$	0.376985	0.36795	0.41754	0.38178
$K_{\varepsilon 3}$	0.417405	0.352428	0.380118	0.355708
$K_{\varepsilon 4}$	0.36107	0.422598	0.359848	0.363233
R_ε	0.056335	0.07017	0.057693	0.02369
K_1	0.732072	0.71838	0.734883	0.688208
K_2	0.717573	0.727187	0.687714	0.713073
K_3	0.687177	0.742151	0.714443	0.738236
K_4	0.732927	0.682031	0.732711	0.730233
R	0.04575	0.06012	0.04717	0.02923

arranged for the obtained parameter plan, and the uniformity index and the imaging relative error were used as the optimization index to obtain the optimized result of the sensor. The optimization results obtained by experimenting with three different structural parameters are shown in Table 4.

TABLE 4. Optimization experiment results.

Optimal group	$A_1B_3C_1D_3$	$A_4B_3C_4D_3$	$A_4B_3C_1D_3$
$T(X)$	4.7302	4.7544	4.6987
ε_{image}	0.34925	0.35775	0.33071

It can be seen from Table 4 that the sensitivity uniformity and image relative error of ECT sensor are improved by using fuzzy comprehensive satisfaction index FCSI as evaluation index, and the structure parameters of capacitance sensor with more uniform distribution of sensitive field and higher image reconstruction quality are obtained.

V. CONCLUSION

This paper uses the method of combining finite element simulation and orthogonal experimental design to optimize the design of ECT sensors, and proposes optimization evaluation indicators based on fuzzy methods, and compares and analyzes the optimization results. The results show:

1) The finite element model of the ECT sensor is constructed in the finite element simulation software, the test scheme is designed by introducing the orthogonal experiment method, the test scheme is arranged efficiently, and the workload is simplified.
2) The experimental results of optimal design of ECT sensor are obtained by orthogonal experimental design. In view of the low sensitivity of the data acquisition system of the electrical capacitance tomography system, the weak detection signal, and other problems, the influence of the structural parameters of the capacitive sensor on the physical performance of the system is analyzed, and the mathematical model of the sensor's sensitive field is established. From the perspective of soft field, Media distribution, the uniformity of the sensitive field and the sensor structure parameters were analyzed, and the optimal design function of the sensor was determined. The fuzzy analysis method of multi-index orthogonal experiment was adopted to obtain a set of sensor optimization parameters, and the sensor optimization design was completed. The results of image reconstruction show that the optimized sensor has high reconstruction accuracy, which is of great significance to the research of ECT system. The variance analysis of the experimental results shows that the weight of the influence on image reconstruction quality from high to low is the relative thickness of the pipeline, the relative height of the shield, the plate angle and the dielectric constant of the insulation material, Make it possible to determine the order of the primary and secondary effects of each factor without passing all the tests.
3) Simulation using COMSOL finite element simulation software, the fuzzy comprehensive satisfaction index FSCI is used as the evaluation index to optimize the parameters of the capacitance sensor. Thickness of the tube wall is 8mm, the height of the shield is 70mm, and the dielectric constant of the filling material is 4. The uniformity of the sensitive field distribution is more uniform and the relative error of the reconstructed image is small, reduce the influence of media distribution., thereby the capacitance measurement can be reconstructed., the final media distribution can reflect the original image more accurately, which proves the rationality and correctness of the method in the multi index ECT sensor parameter optimization. The results of image reconstruction show that the optimized sensor has high reconstruction accuracy, which is of great significance to the research of ECT system. The analysis method is clear, simple and practical, and has universal application value for the analysis of the results of multi-index orthogonal experiments.

REFERENCES

[1] Y. L. Zhou, *Multiphase Flow Parameter Detection Theory and its Application*. Beijing, China: Science Press, 2010.
[2] Q. Marashdeh, L. S. Fan, and B. Du, "Electrical capacitance tomography–a perspective," *Ind. Eng. Chem. Res.*, vol. 47, no. 10, pp. 3708–3719, 2008.
[3] H. J. Tian and Y. L. Zhou, "Research progress of electrical capacitance tomography technology," *Chem. Ind. Autom. Instrum.*, vol. 39, no. 11, pp. 1387–1391, 2012.
[4] Y. Yang and L. Peng, "Data pattern with ECT sensor and its impact on image reconstruction," *IEEE Sensors J.*, vol. 13, no. 5, pp. 1582–1593, May 2013.
[5] Q. Marashdeh, W. Warsito, L.-S. Fan, and F. L. Teixeira, "A multimodal tomography system based on ECT sensors," *IEEE Sensors J.*, vol. 7, no. 3, pp. 426–433, Mar. 2007.
[6] R. Mann, R. A. Williams, T. Dyakowski, F. J. Dickin, and R. B. Edwards, "Development of mixing models using electrical resistance tomography," *Chem. Eng. Sci.*, vol. 52, no. 13, pp. 2073–2085, Jul. 1997.
[7] O. Isaksen and J. E. Nordtvedt, "A new reconstruction algorithm for process tomography," *Meas. Sci. Technol.*, vol. 4, no. 12, pp. 1464–1475, Dec. 1993.
[8] Ø. Isaksen, "A review of reconstruction techniques for capacitance tomography," *Meas. Sci. Technol.*, vol. 7, no. 3, pp. 325–337, 1996.
[9] L. L. Wang, D. Y. Chen, and X. Y. Yu, "Optimal design of electrical capacitance tomography sensor," *Chin. J. Sci. Instrum.*, vol. 36, no. 3, pp. 515–522, 2015.
[10] W. Q. Yang, "Design of electrical capacitance tomography sensors," *Meas. Sci. Technol.*, vol. 21, no. 4, 2010, Art. no. 042001.
[11] Y. G. Zeng, *Electromagnetic Field Finite Element Method*. Beijing, China: Science Press, 1982.
[12] K. H. Tang, H. L. Hu, and L. Li, "A simple method for calculating the sensitivity coefficient of electrical capacitance tomography using field rotation transformation," *J. Xi'an Jiao Tong Univ.*, vol. 53, no. 3, pp. 75–80, 2019.
[13] C. H. Mu, L. H. Peng, and D. Y. Yao, "A calculation method of capacitive imaging sensitivity distribution based on electric potential distribution," *Comput. Phys.*, vol. 23, no. 1, pp. 88–89, 2006.
[14] J. T. Li, S. Liu, and X. Y. Dong, "The design and application of miniature capacitance sensor," *Chin. J. Sci. Instrum.*, vol. 28, no. 8, pp. 1410–1415, 2007.
[15] H. H. Su and Z. J. Yao, "Fuzzy analysis method for multi-index orthogonal test," *J. Nanjing Univ. Aeronaut. Astronaut.*, vol. 36, no. 1, pp. 31–35, 2004.
[16] H. X. Wang, L. F. Zhang, and X. M. Zhu, "Optimal design of array electrodes for electrical capacitance tomography system," *J. Tianjin Univ.*, vol. 36, no. 3, pp. 307–310, 2003.
[17] H. Xu, H. Yan, and E. G. Wu, "The influence of the axial protective plate on the electrical capacitance tomography sensor," *Chin. J. Sci. Instrum.*, vol. 21, no. 2, pp. 159–162, 2010.

ZHE JI (Graduate Student Member, IEEE) was born in Weinan, Shaanxi, in December 1995. He received the B.S. degree in electrical engineering and automation from Weinan Normal University, Weinan, in 2019. He is currently pursuing the master's degree with the School of Automation Engineering, Northeast Electric Power University, Jilin, China.

His main research interests are process detection technology and tomography technology.

JIANYU LIU was born in Songyuan, Jilin, China, in March 1993. He received the B.S. degree in engineering in automation from Beihua University, Jilin, Jilin, China, in 2017, and the M.S. degree in control engineering from Northeast Electric Power University, Jilin, Jilin, China, in 2020, where he is currently pursuing the master's degree with the School of Automation Engineering.

His main research interests are process detection technology and tomography technology.

HAIJUN TIAN (Member, IEEE) was born in Chifeng, Inner Mongolia, China, in April 1971. He received the B.S. degree in production process automation and the M.S. degree in control engineering from Northeast Electric Power University, Jilin, Jilin, China, in 1996 and 2009, respectively, and the Ph.D. degree in thermal engineering from North China University, Beijing, China, in 2019. Since 2008, he has been an Associate Professor with the School of Automation Engineering, Northeast Electric Power University, Jilin, Jilin, China. His main research interests are industrial process modeling and control, process detection technology, and tomography technology.

WANG ZHANG was born in Jilin, Jilin, China, in February 1996. She received the B.S. degree in electrical engineering and automation from the Changchun University of Science and Technology of Changchun, Jilin, in 2018. She is currently pursuing the master's degree with the School of Automation Engineering, Northeast Electric Power University, Jilin.

Her main research interests are process detection technology and tomography technology.